ATTENUATION MEASUREMENTS IN CEMENT-BASED MATERIALS USING LASER ULTRASONICS

By Joseph O. Owino[1] and Laurence J. Jacobs,[2] Member, ASCE

ABSTRACT: This research uses laser ultrasonic techniques to quantify the frequency-dependent attenuation losses of Rayleigh waves in cement-based materials; these materials are heterogeneous in nature, and this heterogeneity is seen at multiple length scales. As a result, ultrasonic waves that propagate in cement-based materials exhibit a high degree of (material) attenuation losses. Physically, these attenuation losses are a combination of internal friction, such as the work done at material interfaces (ultrasonic absorption) and the scattering losses due to material heterogeneity. The high fidelity, large frequency bandwidth, and absolute, noncontact nature of laser ultrasonics makes this an ideal methodology to measure attenuation in these materials. This research uses a dual-probe, heterodyne interferometer to experimentally measure these attenuation losses (as a function of frequency) in three different materials: (1) aluminum; (2) mortar; and (3) granite. The aluminum results (aluminum is homogeneous at the wavelengths used here) are used to demonstrate the fidelity of the laser ultrasonic measurement technique, while the mortar and granite results (both are heterogeneous at these wavelengths) are used to quantify the attenuation losses present in each material.

INTRODUCTION

The use of ultrasonic waves to characterize a material requires the measurement of a variety of wave attributes such as phase velocity and attenuation. For example, experimentally measured phase velocities can be used to calculate elastic constants (such as the Lamé constants λ and μ) while attenuation results can be used to characterize the microstructural properties of a material (such as grain size, porosity, or microcrack distribution). Recent research efforts have developed (and continue to develop) a number of techniques to relate ultrasonic attenuation losses to the microstructure of specific metal and ceramic material systems. However, there is only limited research into the application of these quantitative attenuation techniques to characterize the microstructure of cement-based materials.

The underlying mechanics of the attenuation of ultrasonic waves in cement-based materials (and heterogeneous materials in general) is a difficult problem, with many fundamental questions still unanswered. In addition, it is difficult to experimentally measure attenuation, since the experimental procedure involves the accurate measurement of wave amplitudes as a function of propagation distance and frequency. Potential difficulties with the experimental measurement of attenuation include:

- attenuation measurements are sensitive to the coupling between the transducer and the specimen being tested, a process that can lead to losses that are even greater than the attenuation in the material itself;
- it is often difficult to identify and track a particular portion of an ultrasonic signal (waveform) as a function of propagation distance;
- attenuation measurements require either multiple sources, a truly repeatable source, or multiple receivers; and
- accurate attenuation measurements require high fidelity measurements (no frequency bias) over a broad frequency range.

Few researchers have attempted to measure the attenuation of ultrasonic waves in cement-based materials; this list of research includes work by Tasker et al. (1990), Kim et al. (1991), Gaydecki et al. (1992), and Landis and Shah (1995).

This research uses laser ultrasonic techniques to quantify the frequency-dependent attenuation losses of Rayleigh waves in cement-based materials. The high fidelity, large frequency bandwidth, and absolute noncontact nature of laser ultrasonics makes this an ideal methodology to measure attenuation. In order to demonstrate the accuracy of the proposed attenuation measurements, a reference specimen made of aluminum is examined first. These results exhibit the bandwidth, fidelity, and robustness of laser ultrasonic measurements that are necessary to make accurate attenuation measurements. Next, two different material systems are examined: (1) a mortar specimen; and (2) a granite specimen. These specimens are used as proof-of-principle, demonstration examples of the viability of the proposed measurement technique in cement-based materials.

ATTENUATION MECHANISMS

There are two basic mechanisms by which an ultrasonic wave is attenuated: (1) geometric attenuation; and (2) material attenuation. Geometric attenuation is the phenomenon by which the amplitude of a wave decreases as the wavefront spreads out over a wider area (or volume) as it propagates away from its source. While this is not a true ''loss'' mechanism, it nonetheless causes a decrease in wave amplitude. The amplitude of a plane wave can be written as (Ewing et al. 1957)

$$A(r, f) = \frac{A_o}{r^{\eta}} e^{i(kr - \omega t)} \tag{1}$$

where r = distance from the source; f = frequency; A_o = amplitude at the source; k = wave number; ω = angular frequency ($\omega = 2\pi f$); and the exponent η = geometric attenuation coefficient, which depends on the type of wavefront. Rayleigh surface waves propagate away from the source along cylindrical wavefronts, so the geometric attenuation coefficient (η) in (1) is equal to 0.5; geometric attenuation will cause a decrease in the amplitude of a Rayleigh surface wave of $r^{-1/2}$ as it propagates away from its source. On the other hand, body waves propagate along spherical wavefronts, so their geometric attenuation coefficient (η) is equal to 1.0.

Material attenuation can be classified as either intrinsic (absorption) or extrinsic (scattering). Absorption losses are a result of internal friction due to the work done at material in-

[1]Grad. Res. Asst., School of Civ. and Envir. Engrg., Georgia Inst. of Technol., Atlanta, GA 30332-0355.

[2]Assoc. Prof., School of Civ. and Envir. Engrg., Georgia Inst. of Technol., Atlanta, GA; corresponding author.

Note. Associate Editor: Stuart E. Swartz. Discussion open until November 1, 1999. To extend the closing date one month, a written request must be filed with the ASCE Manager of Journals. The manuscript for this paper was submitted for review and possible publication on September 9, 1998. This paper is part of the ***Journal of Engineering Mechanics***, Vol. 125, No. 6, June, 1999. ©ASCE, ISSN 0733-9399/99/0006-0637–0647/$8.00 + $.50 per page. Paper No. 19187.

terfaces when two materials are not elastically bonded, while scattering losses constitute a highly complex process, which are dependent upon the intrinsic length scale of the scatterer, the number of scatterers per unit volume, the distribution of these scatterers, and the acoustic properties of these scatterers in relationship to the base material. Since these two effects (i.e., absorption and scattering losses) are coupled, attenuation measurements usually include the influence of both the intrinsic and extrinsic effects; it is often impossible to separate the two.

In order to quantify material attenuation, one can introduce the complex form of the wave number, k, as $k = k_r + ik_i$, where k_r is the real part of the wave number, and k_i is the imaginary part of the wave number, referred to as the frequency-dependent attenuation coefficient, $\alpha = \alpha(f)$. Substitution of the complex wave number into (1) yields the following explicit expression for wave amplitude as a function of material attenuation:

$$A(r, f) = \frac{A_o}{r^{\eta}} e^{-\alpha r} e^{i(k_r r - \omega t)} \quad (2)$$

Note that α is the quantitative value for frequency-dependent material attenuation that will be measured in this research.

MICROSTRUCTURE OF CEMENT-BASED MATERIALS

Cement-based materials are heterogeneous (multiphase) composites made up of both coarse and fine aggregates (sand) held together by a binding matrix, usually portland cement. The physical properties of cement-based materials are controlled by several factors including water/cement ratio, type of cement, and curing conditions. A photomicrograph of a typical cross section of mortar is shown in Fig. 1; in this work, mortar consists of fine aggregate (sand), water, and cement (matrix). Fig. 1 provides a graphic illustration of the heterogeneous nature of, and the multiple length scales inherent to cement-based materials. The mix proportions in this specimen are 1.0:2.0:0.40 (cement, sand, and water by weight), and the sand passed through a No. 16 ASTM standard sieve. It is important to note

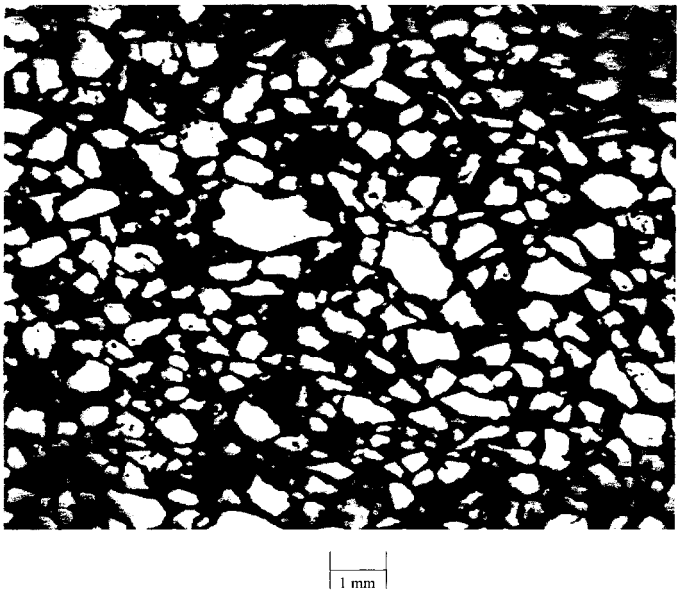

FIG. 1. Photomicrograph of Typical Cross Section of Mortar

that there are other microstructure issues that impact material attenuation in cement-based materials, such as the high level of variability and randomness in the material, and the existence of voids, microcracks, and air bubbles.

This research quantifies material attenuation in two heterogeneous materials: (1) mortar; and (2) granite. The reason for the selection of mortar is that it consists of only two phases (i.e., sand and matrix); mortar is less complicated than ''regular'' concrete (which also includes coarse aggregate) yet it is a true cement-based material. As a result, it is possible to study the intricacies of attenuation losses in cement-based materials without the added complication of coarse aggregate (and an additional length scale). Granite is selected because it is a representative ''natural'' material and it is commonly used as a coarse aggregate.

A critical relationship in the scattering (extrinsic) portion of

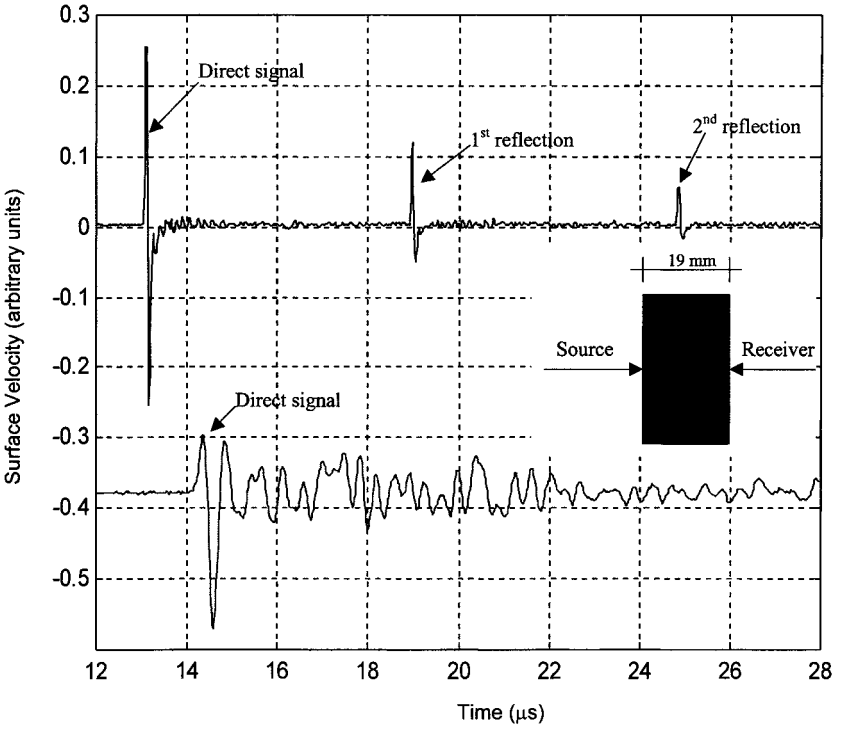

FIG. 2. Comparison of Body Wave that Propagates through 19 mm of Aluminum (Top) and 25 mm of Mortar (Bottom)

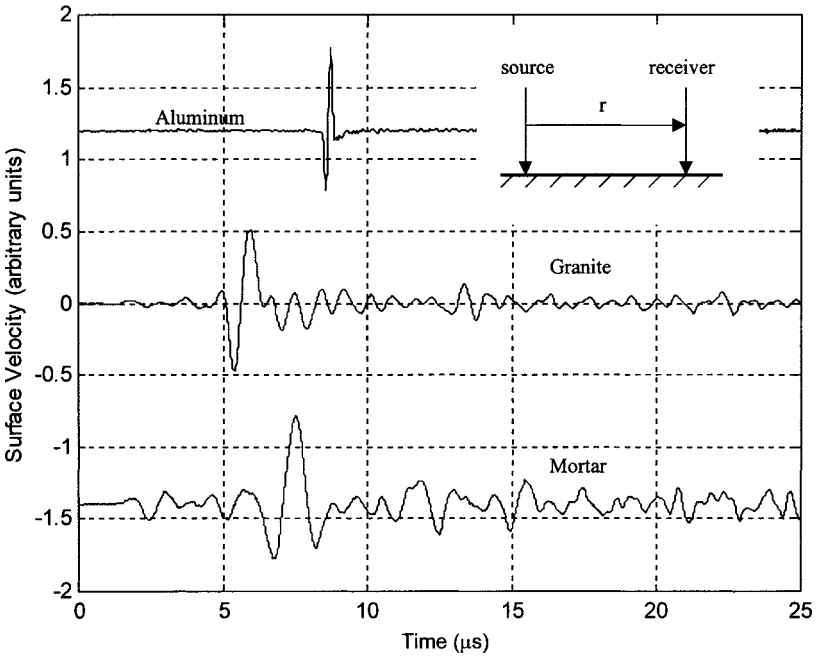

FIG. 3. Comparison of Rayleigh Waves in Aluminum (Top), Granite (Middle), and Mortar (Bottom)

material attenuation is the length scale of the scatterers relative to the wavelength of the ultrasonic waves. The wavelength of a Rayleigh wave is related to its wave speed as $\lambda = C_R/f$, where λ is wavelength, and C_R is the Rayleigh wave speed. Consider the Rayleigh wave speed in mortar (measured in this study) as 2,400 m/s, so the wavelengths of some typical Rayleigh waves are: (1) f of 100 kHz, λ is 24 mm; (2) f of 500 kHz, λ is 4.8 mm; (3) f of 1 MHz, λ is 2.4 mm; and (4) f of 5 MHz, λ is 0.48 mm. In light of the microstructure of mortar (Fig. 1), it is clear that Rayleigh waves with a frequency range of up to 5 MHz provides a wide range of ratios between potential scatterers and Rayleigh wavelengths. As a result, Rayleigh waves with an upper frequency of 5 MHz are broadband enough to investigate the scattering portion of material attenuation in mortar.

EXPERIMENTAL PROCEDURE

Rayleigh surface waves are generated with a Q-switched Nd:YAG laser, using an ablation generation mechanism (Scruby and Drain 1996). The physical principle underlying the laser generation of Rayleigh surface waves is that the electromagnetic energy from the laser pulse vaporizes a few micrometers of the surface of the sample, causing transient stresses that are normal to the surface. These transient stresses generate Rayleigh surface waves, as well as body waves that propagate in a single, broad lobe that is normal to the surface. The Nd:YAG laser used in this study emits a spatially Gaussian profile, with a wavelength of 1,064 nm and a pulse duration of 4–6 ns. The beam diameter that strikes the specimen is regulated using a focusing lens that allows for modifications in the spot size from the laser source. In these experiments, the spot size (source size) is 1 mm in diameter.

Laser detection of Rayleigh waves is accomplished with a dual-probe, heterodyne interferometer that is a modified version of the instrument described in detail by Bruttomesso et al. (1993). This optical device uses the Doppler shift to simultaneously measure out-of-plane surface velocity (particle velocity) at two points on the specimen's surface. The interferometer works by measuring frequency changes in the light reflected off the specimen surface. In a heterodyne interferometer, an artificial frequency shift is initially imposed (using an acousto-optic modulator) to create a reference and a probe beam. The probe beam is reflected off the specimen surface and is recombined with the reference beam at a photodiode. This creates a beat frequency equal to the initial, artificially imposed frequency shift. Frequency shifts in the light reflected from the specimen surface result in proportional shifts in the beat frequency. As a result, the beat frequency signal acts as a carrier that is demodulated in real time (with a frequency modulation discriminator) to obtain the surface velocity. The interferometer makes high fidelity, absolute measurements of surface velocity (particle velocity) over a bandwidth of 10 MHz.

It is important to note that all of the specimens examined in this research have polished surfaces. This preparation enables true noncontact detection (there are no artificial surface treatments such as reflective tape), as well as providing a consistent surface for Rayleigh wave propagation.

Unless otherwise noted, all of the Rayleigh surface waves presented are low-pass filtered at 5 MHz, with the exception of the waveforms measured in the aluminum sample, which are low-pass filtered at 10 MHz. In addition, in order to increase the signal-to-noise-ratio, each waveform presented represents a collection of averages, sometimes as many as 100. This signal averaging procedure works because noise is ran-

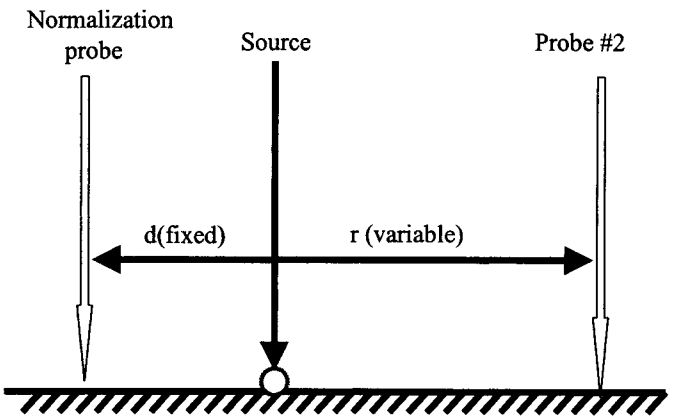

FIG. 4. Schematic of Experimental Setup for Multistation Measurements

dom and will average out, while the ''real'' signal is repeatable and is unaffected by averaging.

ATTENUATION MEASUREMENTS USING RAYLEIGH WAVES

This research uses laser ultrasonic techniques to make in situ measurements of frequency-dependent attenuation in cement-based materials. The heterogeneous and random nature of cement-based materials dictates the selection of Rayleigh surface waves (as opposed to body waves, such as longitudinal or shear waves) for this application.

There are two main reasons for the selection of Rayleigh waves. First, the attenuation of a body wave is usually measured by comparing the initial (direct) wave amplitude that propagates through one thickness of the specimen, to the reflected wave amplitude that propagates through three thicknesses of the specimen; this requires a clearly identifiable wave that reflects from the back surface. In a homogeneous material, like a metal, this reflected wave is easily identified. Unfortunately, this is not the case for a (heterogeneous) cement-based material. Fig. 2 provides a qualitative illustration of the difficulty, if not absurdity, of trying to directly measure the attenuation of body waves in cement-based materials using this reflected wave; Fig. 2 compares the longitudinal waves (generated and detected using laser ultrasonics, with source

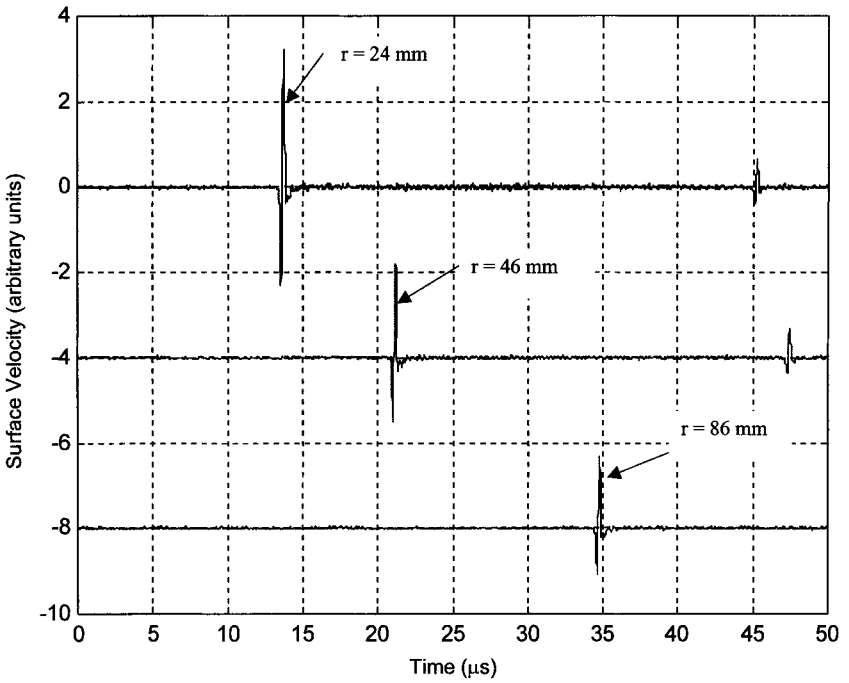

FIG. 5. Typical Rayleigh Waveforms Measured in Aluminum with Multistation Method at *r* = 24 mm (Top), *r* = 46 mm (Middle), and *r* = 86 mm (Bottom)

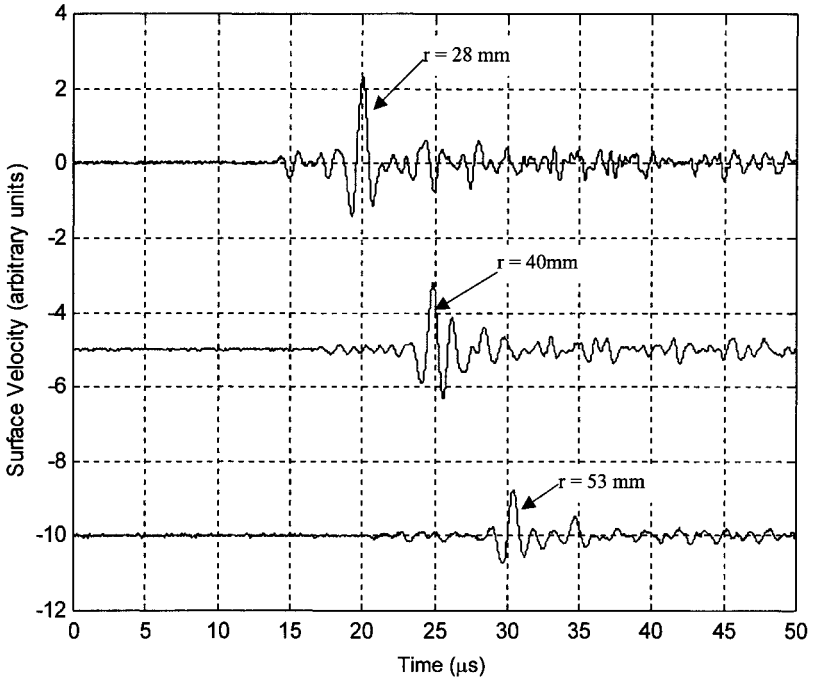

FIG. 6. Typical Rayleigh Waveforms Measured in Mortar with Multistation Method at *r* = 28 mm (Top), *r* = 40 mm (Middle), and *r* = 53 mm (Bottom)

and receiver on opposite sides of the specimen) that have propagated through 19 mm of aluminum and 25 mm of mortar. The direct wave, as well as two multiple reflections from the back surface are clearly discernible in the 19 mm thick aluminum sample, while only the initial (direct) arrival is identifiable in the mortar sample. What has happened in the mortar sample is that the initial signal (wave) is scattered by the mortar's (heterogeneous) microstructure, thus hiding the wave reflected off the back surface.

The second reason for using Rayleigh waves in this research is that it is relatively easy to design an experimental procedure that measures changes in Rayleigh wave amplitude as a function of propagation distance for a Rayleigh wave that propagates through exactly the same material volume. This procedure entails keeping the source in a constant location, while the receiver is moved incremental distances along a straight line. This multistation method, which is described in detail in a later section, is only possible for body waves when multiple specimens, each with a different thickness (and, thus, propagation distance), are available. Unfortunately, with multiple specimens, the body wave propagates through a different volume of material for each measurement. As a result, changes in waveform amplitude due to the inherent variability present in cement-based materials will dominate these measurements, causing erroneous attenuation results.

Attenuation analysis (unlike wave velocity measurement) involves the accurate measurement of wave amplitudes as a function of propagation distance and frequency. Any inconsistency in the ultrasonic source will result in inconstant wave amplitudes, which will cause errors in the attenuation calculations. This research uses a dual-probe interferometer to ensure that the laser source generates wave amplitudes that are truly constant. The second probe (receiver) enables an independent, quantitative measure of each wave amplitude (as a

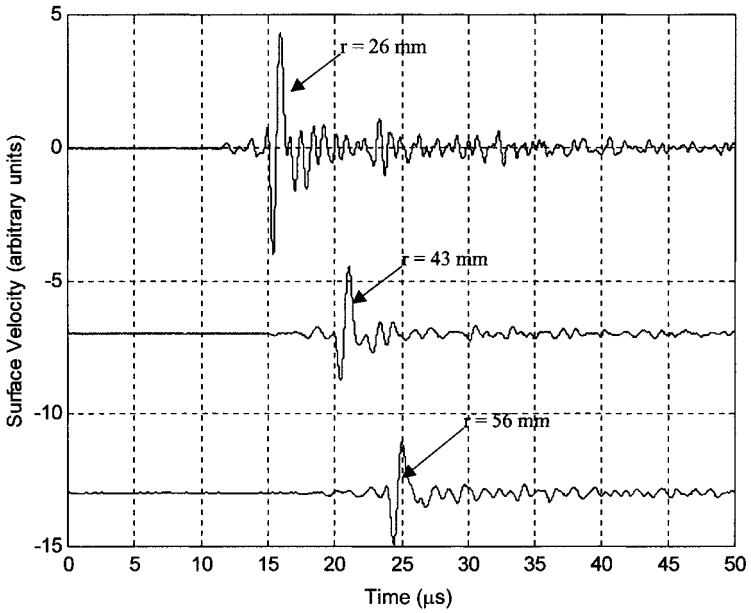

FIG. 7. Typical Rayleigh Waveforms Measured in Granite with Multistation Method at *r* = 26 mm (Top), *r* = 43 mm (Middle), and *r* = 56 mm (Bottom)

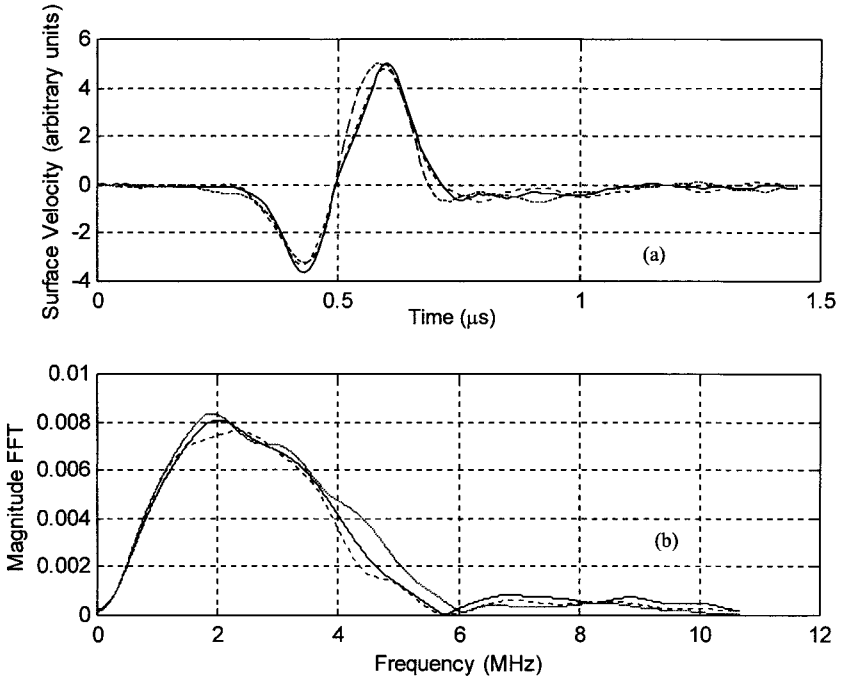

FIG. 8. 1.5 μs Window for Aluminum: Time and Frequency Domain

function of frequency) and provides a normalization value that is used to remove slight variations is source strength (Appendix I).

QUALITATIVE COMPARISON OF RAYLEIGH SURFACE WAVES IN ALUMINUM, GRANITE, AND MORTAR

Fig. 3 shows typical Rayleigh surface waves (generated and detected using laser ultrasonics) in aluminum, granite, and mortar specimens; each of these waves has propagated approximately the same distance (26 mm). Each of these specimens is nominally a cube of 150 × 150 × 150 mm. The most interesting feature revealed in Fig. 3 is the enormous amount of ultrasonic scattering (following the arrival of the Rayleigh wave) in granite and mortar that is absent in the aluminum. This is not surprising since at these ultrasonic wavelengths, aluminum is a homogeneous material while the other samples are heterogeneous. It is also interesting to note the amount of deviation between these three waveforms, even though each is generated with exactly the same Nd:YAG laser pulse. It is clear that an ultrasonic waveform generated with an laser source is directly dependent upon the material being interrogated; this is not the case for generation with a piezoelectric transducer. A final point is that the longitudinal wave arrival that propagates along the surface is clearly visible in the granite and mortar samples, while it is virtually absent in the waveform measured in aluminum. This disparity is attributed to differences in the laser source; light from the Nd:YAG pulse

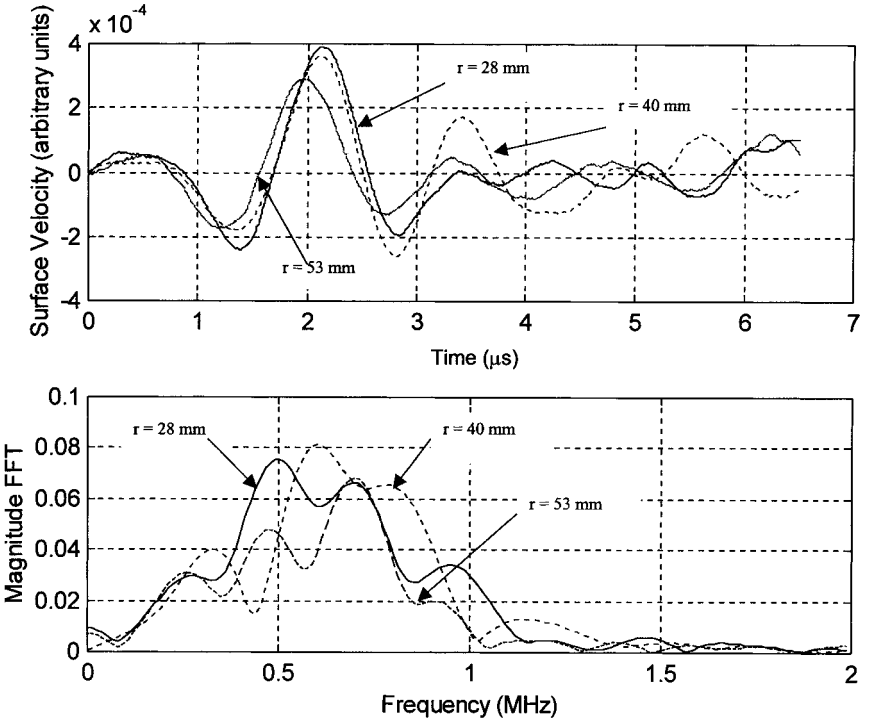

FIG. 9. 6 μs Window for Mortar: Time and Frequency Domain

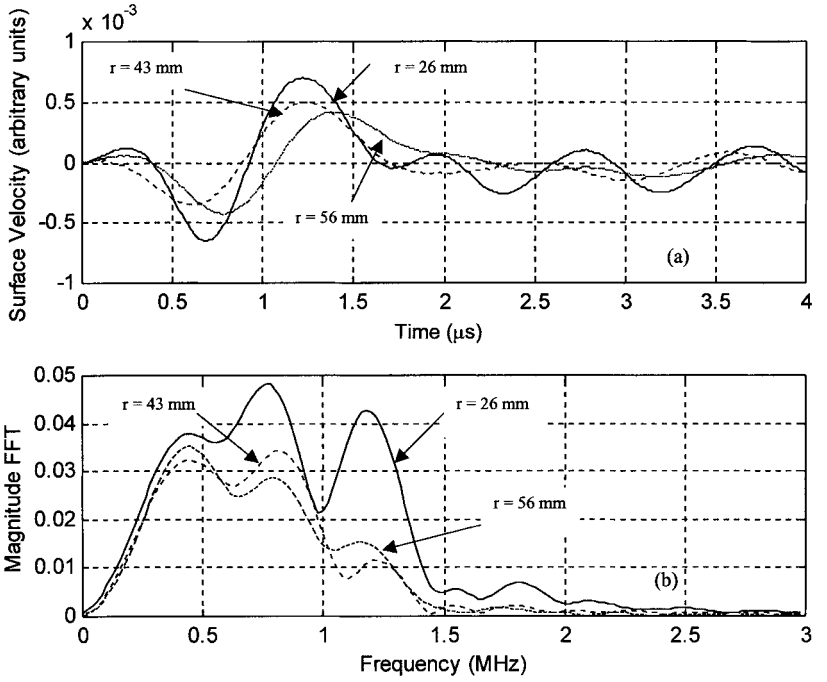

FIG. 10. 4.5 μs Window for Granite: Time and Frequency Domain

penetrates further into the granite and mortar, thus creating more of a buried source.

MEASUREMENT OF FREQUENCY-DEPENDENT ATTENUATION USING MULTISTATION METHOD

In the multistation method, one receiver (the normalization probe) is located at a fixed distance, *d*, from the source, while the second receiver (probe #2) is located at a variable (propagation) distance, *r*, from the source (Fig. 4). A Rayleigh surface wave is generated and detected in this position, and then probe #2 is moved a prescribed distance (with a micrometer) away from the source (along a line on the surface of the specimen), and the procedure is repeated. Note that while the position of probe #2 changes, the locations of both the source and the normalization probe remain the same throughout the entire procedure. As a result, the normalization probe ensures that each waveform detected by probe #2 is due to exactly the same source; source repeatability is discussed in detail in Appendix I.

Application of the multistation method yields the following results. Figs. 5–7 show three typical Rayleigh waves, each measured with probe #2 at three different propagation distances, *r*, in the aluminum, mortar, and granite specimens. The dispersive nature of granite and mortar is qualitatively visible by the change in shape of the Rayleigh waves in the upper waveforms (closer propagation distances) when compared to the lower waveforms (farther propagation distances). This dispersion is clearly not present in the aluminum specimen; all the aluminum waveforms have the same shape, no matter what the propagation distance. Note that dispersion is the process by which different frequencies propagate with different phase velocities, causing a change in shape as a wave ''pulse'' propagates. The material dispersion present in Rayleigh waves measured in the granite and mortar specimens is due to the heterogeneous nature of their microstructures.

In order to better understand Rayleigh wave propagation in cement-based materials, the waveforms measured with the multistation method are examined in more detail. A rectangular window is used to isolate the contribution of just the Rayleigh portion of each waveform and to track changes in the time and frequency domains.

As a reference, first consider the aluminum specimen. Fig. 8(a) shows the 1.5 μs (rectangular) window that includes the Rayleigh portion of three typical waveforms with different propagation distances (and shifted to remove the time delays). Note that geometric attenuation (losses due to spreading originally present in each of these waves) has been removed by multiplying each wave by the square root of its respective propagation distance, *r*. Fig. 8(a) also shows that once geometric attenuation is removed, each of these Rayleigh waves is nearly identical; this is further proof that material attenuation in aluminum (losses due to scattering and absorption) is negligible—aluminum is nondispersive in this frequency range. The frequency content of these Rayleigh waves is calculated by taking the fast Fourier transforms (FFTs) (padded to the original sampled length, 15,000 points) of each wave in Fig. 8(a). The magnitude of the FFT of each of these Rayleigh waves is shown in Fig. 8(b). Since the three FFTs in Fig. 8(b) are nearly identical to each other, Fig. 8(b) demonstrates that the frequency content of a Rayleigh wave measured in aluminum is not dependent on its propagation distance. Again, this result is expected, since there are no frequency-dependent scattering or absorption losses present.

Fig. 8(b) also illustrates a critical feature of this research; the high fidelity and broadband nature of laser ultrasonics. The laser ultrasonic techniques used in this work can accurately measure (without bias) Rayleigh waves over a very wide frequency bandwidth (up to 10 MHz). As a result, these techniques can be used to precisely track small changes in frequency that may be present in Rayleigh waves.

Next, consider the mortar and the granite specimens. Fig. 9(a) shows the 6 μs rectangular window that includes the Rayleigh portion of three typical waveforms measured in mortar, while Fig. 10(a) shows three typical granite (4.5 μs window) Rayleigh waveforms. Note that as in Fig. 8(a), geometric attenuation has been removed by multiplying each wave by the square root of its respective propagation distance. The dispersive nature of these waves is qualitatively demonstrated by the fact that the waveforms in Figs. 9(a) and 10(a) are different from each other, even after geometric attenuation has been removed. This is proof that material attenuation, due to scattering and absorption in mortar and granite, is not negligible in this frequency range. As before, the frequency content of

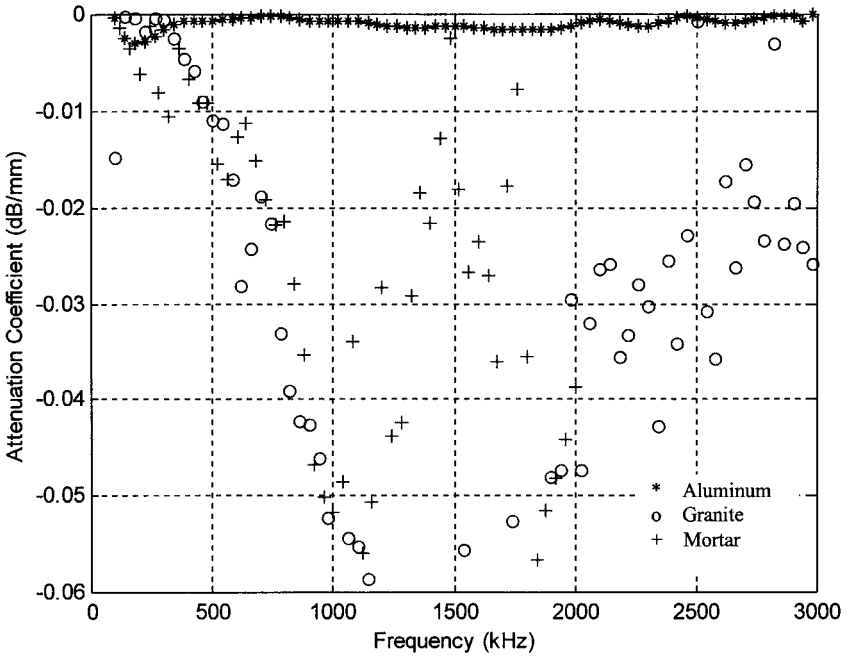

FIG. 11. Plot of Frequency-Dependent Attenuation Coefficient, α, versus Frequency for Aluminum, Mortar, and Granite

these Rayleigh waves is calculated by taking the FFTs of each padded wave in Figs. 9(a) and 10(a); the magnitude of these FFTs are shown in Figs. 9(b) and 10(b). A qualitative manifestation of the frequency-dependent scattering and absorption losses present in both mortar and granite is the fact that the three FFTs in Fig. 9(b), and the three FFTs in Fig. 10(b), are different from each other; the frequency content of a Rayleigh wave measured in either mortar or granite is dependent on its propagation distance. These frequency-dependent losses are quantified by calculating the frequency-dependent attenuation coefficient, α, defined in (2).

The frequency-dependent attenuation coefficient, α, is calculated by comparing the geometrically corrected frequency spectrum measured at a number of propagation distances, r_1, r_2, . . . , r_n (probe #2) to that of a reference spectrum (the normalization probe in this study). The step-by-step procedure used to calculate α is

- The time domain waveforms (measured r_1, r_2, . . . , r_n) are windowed and transformed into the frequency domain. Denote the transformed signals as $A_i(f)$ for distance r_i and as $A_{ref}(f)$ for the normalization probe.
- Remove geometric attenuation in both $A_i(f)$ and $A_{ref}(f)$ by multiplying by the square root of their respective propagation distances. Denote the geometrically corrected signals as $\overline{A_i}$ and $\overline{A_{ref}}$.
- Normalize the geometrically corrected $\overline{A_i}$ with a point-by-point division with the geometrically corrected reference spectra ($\overline{A_{ref}}$) or $A^* = \overline{A_i}/\overline{A_{ref}}$.
- Plot ln (A^*) against propagation distances r_i, at a discrete

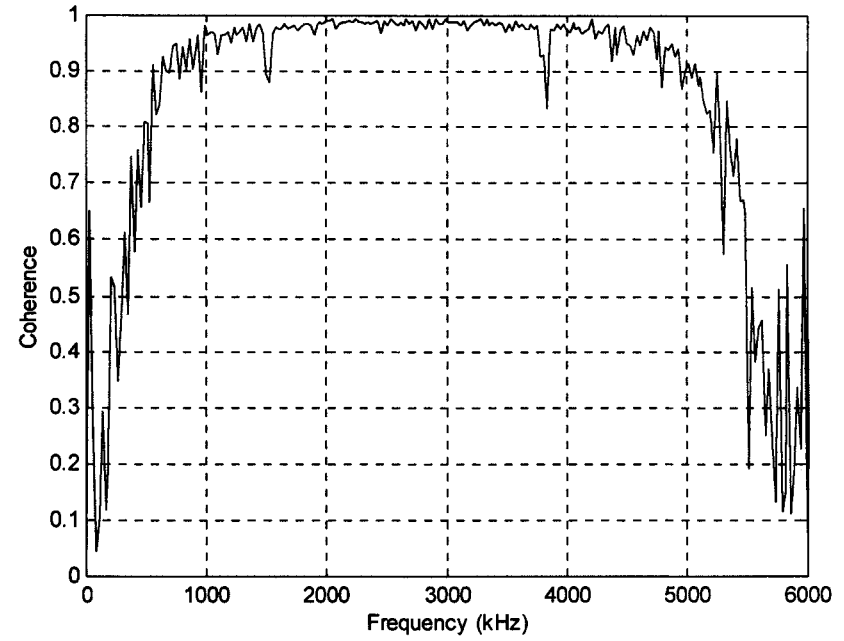

(a)

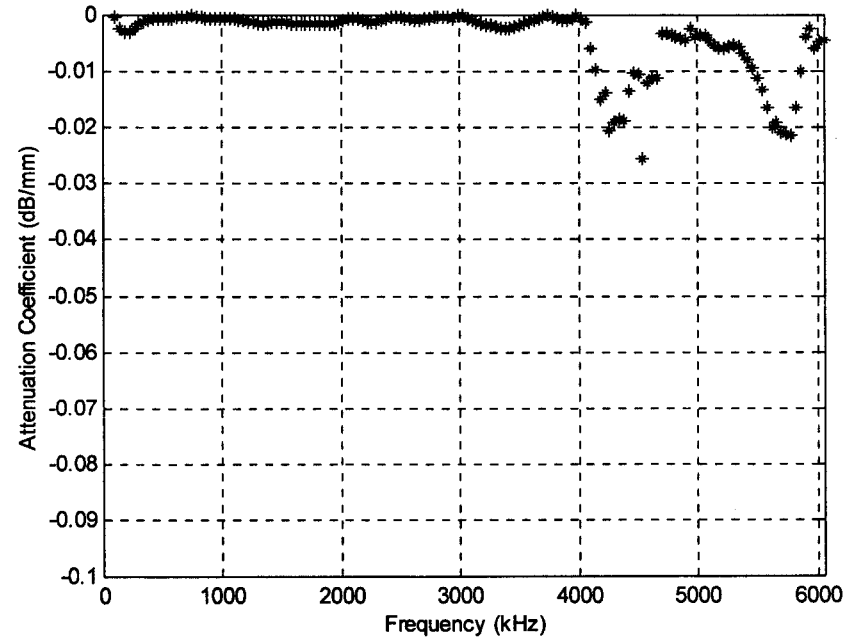

(b)

FIG. 12. Coherence and Frequency-Dependent Attenuation Coefficient, α, versus Frequency for Aluminum

number of frequencies, f_1, f_2, . . . , f_n. Perform a linear regression analysis at each discrete frequency, and the slope of the regression analysis is the attenuation coefficient, $\alpha(f_i)$, at that discrete frequency, f_i.

This method is used to calculate the frequency-dependent material attenuation coefficients for the aluminum, mortar, and granite specimens, and the resulting α versus f values are shown in Fig. 11. For example, the α measured in mortar (Fig. 11) is calculated using 15 waveforms (at 3 mm separation intervals) and with 48 discrete frequencies, from 100 kHz to 3 MHz (at 40 kHz intervals). Fig. 11 shows that aluminum exhibits virtually no material attenuation up to 3 MHz, while there is a high degree of scatter in the mortar and granite results. A qualitative interpretation of the mortar results shows a generally linearly increasing trend up ~1 MHz, followed by a decrease (or random pattern) in α, while granite is increasing linearly to a frequency of ~1.4 MHz, followed by the same behavior as mortar (for the higher frequencies). A more quantitative interpretation of these results is possible using the concept of coherence.

COHERENCE ANALYSIS

An important criteria in determining the accuracy of attenuation measurements is coherence, a frequency-dependent measure of the linearity of attenuation measurements. Coherence is defined as the fractional portion of the output signal (the measured Rayleigh surface wave in this case) that is due to the input signal (the laser source in this case) at a specific frequency, f. Coherence is especially helpful in determining

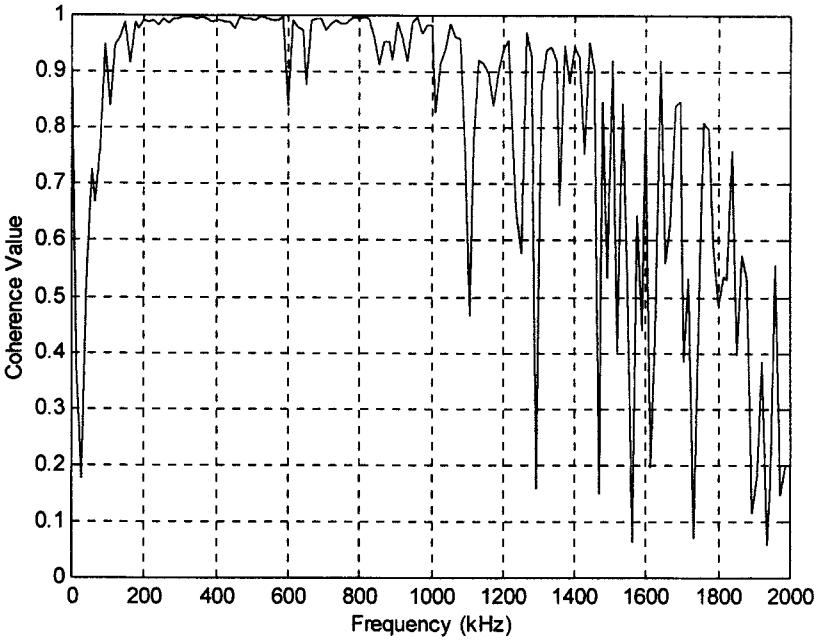

(a)

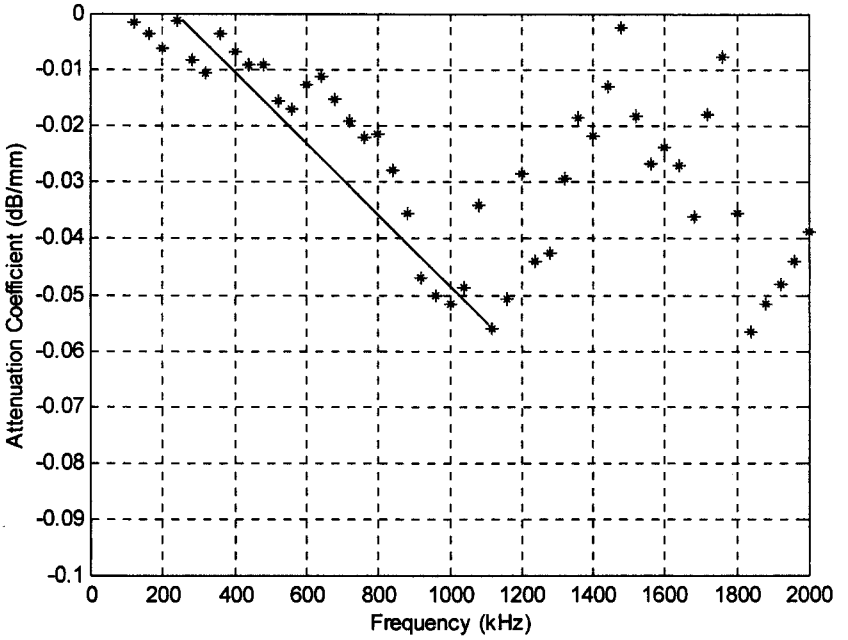

(b)

FIG. 13. Coherence and Frequency-Dependent Attenuation Coefficient, α, versus Frequency for Mortar

the frequency bandwidth through which an experimentally measured attenuation coefficient (α) is reliable. A coherence value of 1 indicates perfect coherence between the input output signal (100% of the output is due to the input), while a coherence of <1 indicates either excessive noise or a nonlinear response at a specific frequency. Frequency components whose coherence values are <0.9 are usually rejected.

Define coherence as (Santamarina and Fratta 1998)

$$\gamma^2(f) = \frac{\left(\left|\sum V(r_2 f)\cdot \overline{V}(r_1 f)\right|\right)^2}{\left(\sum V(r_1 f)\cdot \overline{V}(r_1 f)\right)\cdot\left(\sum V(r_2 f)\cdot \overline{V}(r_2 f)\right)} \quad (3)$$

where γ = coherence; $V(r_1 f)$ = velocity spectra measured at propagation distance r_1; and $\overline{V}(r_2 f)$ = complex conjugate of the velocity spectra measured at propagation distance r_2.

The dual-probe interferometer is reconfigured so that the probes are at two fixed propagation distances (r_1 and r_2) from the laser source. Equation (3) is then applied to waveforms measured with the new configuration in the aluminum, mortar, and granite samples. The coherence for each of these three samples is shown in Figs. 12–14, together with their respective attenuation coefficient values, α (the same α values as presented in Fig. 11).

Figs. 12–14 show that coherence is a quantitative tool that enables an accurate interpretation of experimentally measured material attenuation. For example, the coherence results for

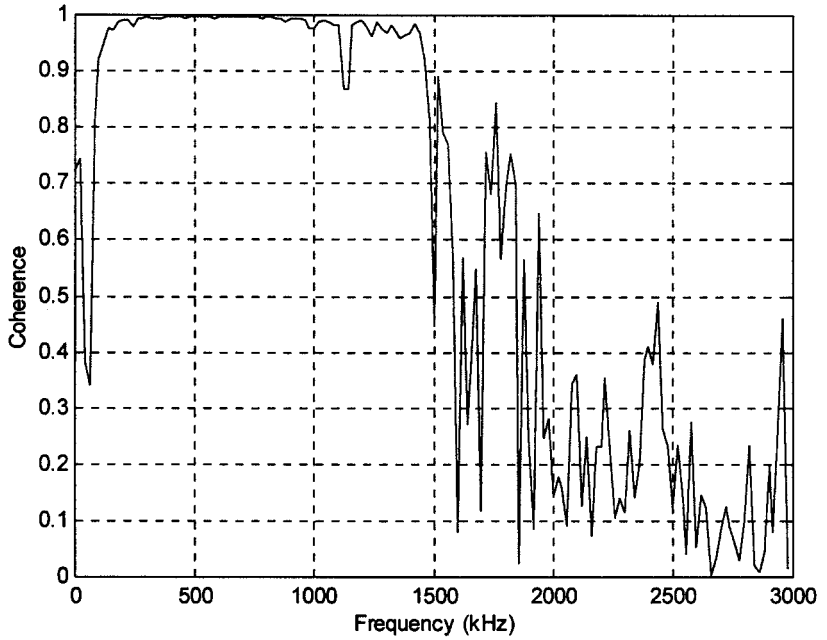

(a)

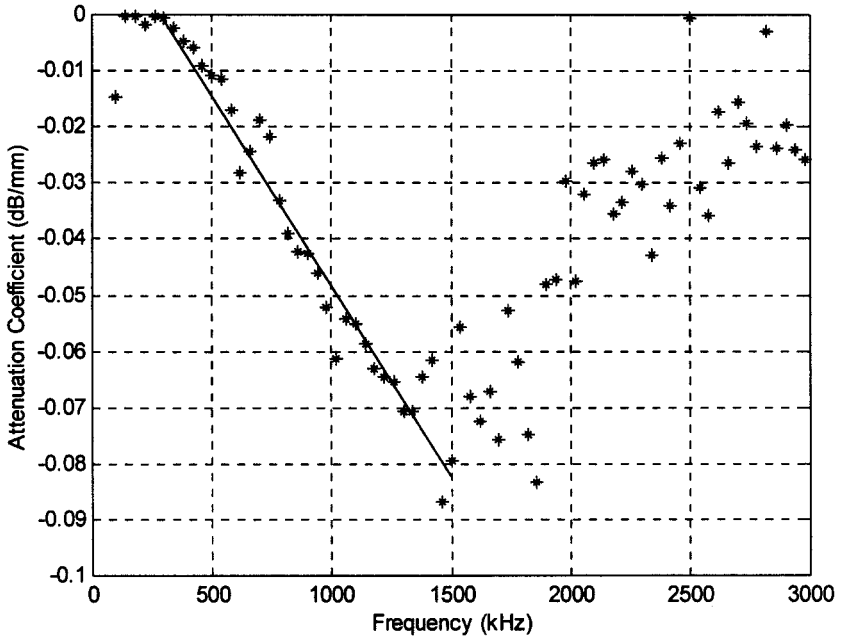

(b)

FIG. 14. Coherence and Frequency-Dependent Attenuation Coefficient, α, versus Frequency for Granite

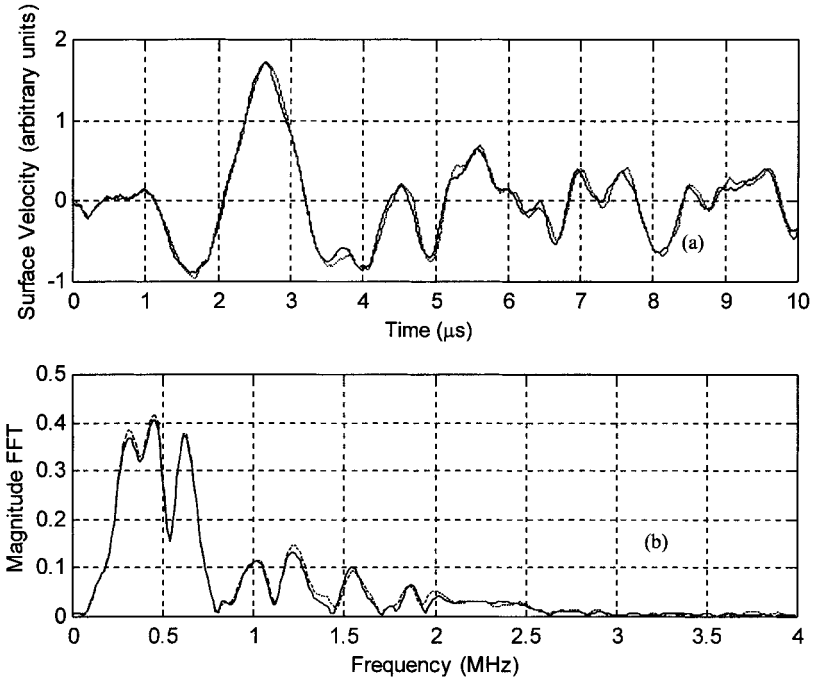

FIG. 15. Repeatability of Two Typical Normalization Probe Plots in Mortar: Time and Frequency Domain

the aluminum specimen indicate that attenuation values above a frequency of ~5 MHz should be rejected, corresponding very well to the frequency value when these attenuation results begin to exhibit a degree of random scatter. The same trend holds true for the mortar and granite specimens. The coherence results for mortar indicate that attenuation values above 1 MHz should be rejected, while the coherence results for granite indicate a reliable upper frequency of 1.4 MHz. It is important to note that these coherence results mimic the behavior of the FFTs presented in Figs. 8(b)–10(b). For example, Fig. 9(b) shows that there is very little signal above 1 MHz in the mortar specimen. The coherence results justify eliminating all the attenuation coefficients above 1 MHz for mortar and 1.4 MHz for granite, and fitting a straight line to the remaining values; these lines are shown on Figs. 13 and 14.

CONCLUSION

This research demonstrates the effectiveness of using laser ultrasonic techniques to quantify attenuation losses in cement-based materials. By using this state-of-the-art technology, it is possible to experimentally measure the frequency-dependent material attenuation coefficient, α, over a broad frequency bandwidth. It is critical to note that these experimental measurements are only possible because of the high fidelity, unbiased, broadband, point source/point receiver, and noncontact nature of laser ultrasonics.

These results further the comprehension of the underlying mechanics of ultrasonic wave attenuation in cement-based materials (and heterogeneous materials in general). This research provides benchmark experimental results measured with an accurate, reliable, and consistent procedure. In addition, this work shows that the frequency-dependent material attenuation coefficient, α, is linear within the range of valid coherence values.

The next step is to relate these ultrasonic attenuation losses to the microstructure of the specific cement-based material being interrogated. This will enable the use of these quantitative attenuation techniques to characterize the microstructure of cement-based materials. Potential applications include measurement of porosity or tracking the growth of microcracks in a (surface) volume of mortar.

APPENDIX I. REPEATABILITY OF LASER SOURCE

For this research to be successful, it is imperative to have a consistent (repeatable) source; the normalization probe ensures that the laser source provides a constant waveform with little or no variations. Causes of variation include either surface damage or local variations in the material at the source (this is a major issue with heterogeneous materials). A measure of source repeatability comes from an examination of the entire time and frequency domain signals measured by the normalization probe. Fig. 15 shows two ''typical'' Rayleigh surface waves measured by the normalization probe in the mortar specimen; each waveform is generated by a different source. Note that for brevity, the results from the normalization probe in the aluminum and granite specimens are not included since they show the same trends as the mortar results. Each of the two typical mortar waveforms (Fig. 15) are nearly identical to each other, in both the time and frequency domains, showing that laser generation of ultrasound provides a repeatable source for these attenuation measurements.

APPENDIX II. REFERENCES

Bruttomesso, D. A., Jacobs, L. J., and Costley, R. D. (1993). ''Development of an interferometer for acoustic emission testing.'' *J. Engrg. Mech.*, ASCE, 119(11), 2303–2316.

Ewing, M., Jardetzky, W., and Press, F. (1957). *Elastic waves in layered media*. McGraw-Hill, New York.

Gaydecki, P. A., Burdekin, F. M., Damaj, W., Johns, D. G., and Payne, P. A. (1992). ''The propagation and attenuation of medium-frequency ultrasonic waves in concrete: A signal analytical approach.'' *Measurement Sci. and Technol.*, 3(1), 126–134.

Kim, Y. H., Lee, S., and Kim, H. C. (1991). ''Attenuation and dispersion of elastic waves in multi-phase media.'' *J. Physics, D: Appl. Physics*, 24(10), 1722–1728.

Landis, E. N., and Shah, S. P. (1995). ''Frequency-dependent stress wave attenuation in cement-based materials.'' *J. Engrg. Mech.*, ASCE, 121(6), 737–743.

Santamarina, J. C., and Fratta, D. (1998). *Discrete signals and inverse problems in civil engineering*, ASCE, Reston, Va.

Scruby, C. G., and Drain, L. E. (1990). ''Laser Ultrasonics: Techniques and applications.'' Adam Higler, New York.

Tasker, C. G., Milne, J. M., and Smith, R. L. (1990). ''Recent work at the National NDT Centre on concrete inspection.'' *British J. NDT*, 32(7), 355–359.